FASTC-ID(RS)T-0331-93

(2)

FOREIGN AEROSPACE SCIENCE AND TECHNOLOGY CENTER

ANALYSIS OF A SANDSTORM WEATHER PROCESS

by

Yang Dongzhen, Ji Xiangming, et al.

HUMAN TRANSLATION

FASTC-ID(RS)T-0331-93 5 November 1993

MICROFICHE NR: 93C000643

ANALYSIS OF A SANDSTORM WEATHER PROCESS

By: Yang Dongzhen, Ji Xiangming, et al.

English pages: 19

Source: Yici Huangsha Tianqi Guocheng Di Fenxi, QIXIANG XUEBAO [METEOROLOGY], Vol. 49, No. 3, August 1991; pp. 334-342

Country of origin: China
Translated by: Leo Kanner Associates
F33657-88-D-2188
Requester: USAF Environmental Technical Applications Center/Robert A. Van Veghel
Approved for public release; Distribution unlimited.

THIS TRANSLATION IS A RENDITION OF THE ORIGINAL FOREIGN TEXT WITHOUT ANY ANALYTICAL OR EDITORIAL COMMENT STATEMENTS OR THEORIES ADVOCATED OR IMPLIED ARE THOSE OF THE SOURCE AND DO NOT NECESSARILY REFLECT THE POSITION OR OPINION OF THE FOREIGN AEROSPACE SCIENCE AND TECHNOLOGY CENTER.	PREPARED BY: TRANSLATION DIVISION FOREIGN AEROSPACE SCIENCE AND TECHNOLOGY CENTER WPAFB, OHIO

GRAPHICS DISCLAIMER

All figures, graphics, tables, equations, etc. merged into this translation were extracted from the best quality copy available.

STOP HERE

ANALYSIS OF A SANDSTORM WEATHER PROCESS

Yang Dongzhen, Ji Xiangming, Xu Xiaobin, Fu Jimeng, and Wen Yupu

Academy of Meteorology Science, State Meteorology Administration

Abstract

The favourable synoptic situation and climate background for a sandstorm process, which occurred in the period from the 9th to the 16th of April 1988, has been studied through analyzing weather maps, meteorological elements, satellite cloud pictures and sandstorm trajectories. The sand dust origin area, the directions and the paths of sand dust transportation and the extent the sand dust reached were also investigated. The results of measurments and analysis indicate that the concentration of sand dust particles is 10 times greater than the normal. It is also shown that the elements in the sand dust are lithophile and come from natural source through the chemical composition analysis of the sand dust, so that the sand dust has not been seriously polluted by human activities.

I. Foreword

The so-called sandstorm weather process can be defined as a large scale weather process of sandstorms, floating dust and blown sand caused by atmospheric weather. Following a high altitude westerly belt, these weather phenomena can move eastward to as far as Japan or even the Northern Pacific.

Since the climatology effect caused by the sandstorm weather process (such as atmospheric visibility, optical features of the

atmosphere, ground-atmosphere radiation equilibrium) can influence and damage the natural ecological environment, These factors constitute one of the atmospheric and ecological environmental problems that cannot be ignored. Therefore, the problem has attracted the attention of scholars in China and abroad for a long time; a considerable amount of study has been conducted. For example, at the Mauna Loa Background Monitoring Station (established by the NOAA of the United States) on the Island of Hawaii, close attention and monitoring of East Asia dust storms and their effect on the station, as well as the physicochemical features of dust-air sol have been analyzed and studied for a long time [1]. In Japan, 21 dust storms from East Asia from 1982 through 1988 were analyzed and summarized by using meteorological satellite cloud pictures. The Japanese researchers call it KOSA (dust cloud or dust storm); the place of origin, influence areas and the subsidence amount of sand and dust in the transport process of a dust storm [2] were estimated [2]. In addition, some researchers in Japan further pointed out the importance of KOSA with respect to terrestrial chemical circulation of soil microparticles [3]. Such studies were also conducted by many units in China. For example, detailed explorations and studies were made by the Institute of Atmosphere and Institute of High Energy Physics of the Chinese Academy of Sciences at the place of origin of dust storms, as well as characteristics of sand and dust [4].

In Northwest China, there are large expanses of desert and gobi in addition to a loess plateau which is the thickest loess belt on the globe. Under certain climate background and weather situations every spring, sandstorm (or, as some say, dust storm) weather can easily occur. In this article, analyses and studies are conducted on the weather situation of the intensive sandstorm weather processes as from 9 to 16 April 1988, along with the place of origin (and some physicochemical characteristics) of sand and dust, transport routes, as well as some physicochemical

characteristics.

II. General Conditions and Weather Situation of Sandstorm Weather Process From 9 to 16 April 1988

1. General situation

This sandstorm weather process began at 20.00 hours on 9 April. First, a gale and sandstorm occurred at Urumqi. With movement of the frontal surface toward the east and south, the gale and sandstorm followed the front. At 20.00 hours on 12 April, the scope of sandstorm weather covered as far south as Changsha and Guilin, as far west as Nanchong and Daxian, and as far east as Shanghai and Hangzhou (see Fig. 1). On 13 April, the sandstorm began weakening, and disappeared quickly in areas north of the Huai River. On 14 April, the sandstorm basically disappeared except over a few southern cities, such as Guilin. The entire weather process ended on 16 April. As the weather phenomena occurred, there was floating dust in the south; mainly, there were sandstorms and blown sand in the areas of Xinjiang, Inner Mongolia and the loess plateau in North China, as well as areas of these plains with extremely bare ground surface. The phenomena are related to gravity subsidence of sand, long distance transport, and conditions of the ground surface being filled underneath.

2. Weather situation

On the 500 hPa map at 08.00 hours on 6 April, there was a large trough in northeast Europe; over the western portion of Novaya Zemlya, an intensive cold center (-43°C) paired with the trough, which moved eastward and reached the Chinese terrotory at 20.00 hours on 9 April. With the invasion of a cold (air) front, a gale and sandstorm occurred over Urumqi, Xinjiang. At 08.00 hours on 10 April, another deep trough in western Europe successively moved eastward, thus greatly intensifying the entire weather process. At the same time, a polar front was hampered by

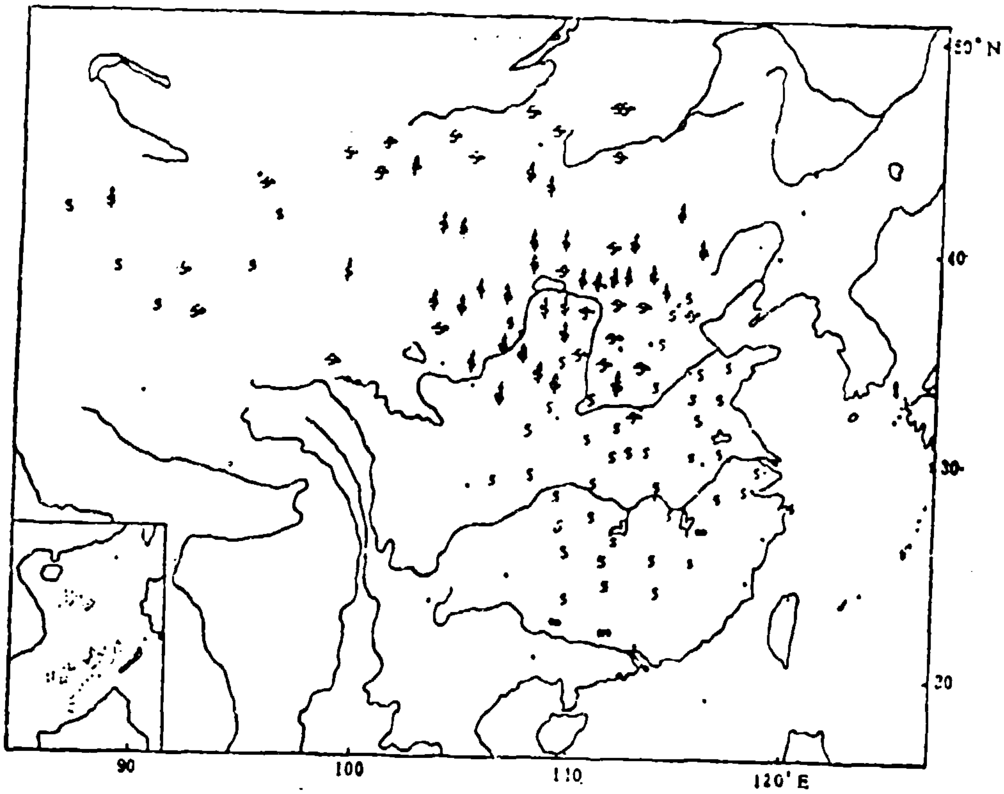

Fig. 1 Distribution of sandstorms, blown sand and floating dust over China from 20.00 hours on 9 April to 20.00 hours on 12 April in 1988

high pressure in southern Europe, and split into two branches: south and north. Both branches moved eastward to eastern Xinjiang, Inner Mongolia and the western loess plateau, and then merged. Thus, cold air intensively erupted; large amounts of sand and dust swirled up with the wind. At 20.00 hours on 10 April, the cold front reached central Inner Mongolia as well as the middle and upper reaches of the Yellow River. At 14.00 hours on 11 April, the front surface moved to the eastern portion of North China, and western portions of the Yangtze and Huai Rivers. At 08.00 hours on 12 April, the front entered eastern China and South China Sea. In areas passed by the front, gales and gusts of wind occurred, frequently with flying sand, dust, sandstorms

and floating dust with a sudden drop of visibility to only 0.1 kilometer at the lowest point.

At 08.00 hours on 12 April, there were large expanses of air flow (from northwest) behind the 500 and 700 hPa troughs. However, along the lines of Nanjing, Wuhan, Nanchang, Changsha and Guilin of the 850 hPa trough, there was intensive air flow (from northeast) with wind speed as high as 12 to 14 meters per second. Thus, some sand and dust turned southwestward. As a result, a weather phenomenon of floating dust successively occurred from 14.00 hours on 12 April to 14.00 hours on 14 April over Changsha and Guilin.

III. Tracing Backward to the Place of Origin of Sand and Dust

1. Analysis on locus of sand and dust

The locus of sand and dust was calculated according to the revised Euler method [5] proposed by Harris.

First, according to 12 hour intervals of the wind speed component, calculate by interpolating the mean wind velocity for every three hour interval based on the following formula.

$$x_{i,j}=\frac{x_{i,j}(t_{12})-x_{i,j}(t_0)}{12}\times\tau+x_{i,j}(t_0)$$

In the formula, $x = u, v$, $\tau = 1.5, 4.5, 7.5$ and 10.5
i and j are coordinates of the lattice point; t_0 and t_{12} represent, respectively, the time of two analyzed fields; the length of time step is 3 hours. The data of wind speed are taken from geostrophic wind calculated from an altitude field and objectively analyzed at the State Meteorology Center.

Generally, the locus calculation is as follows: from wind speed data of two objective analyses every day, compute by interpolating the wind velocity for three hour intervals (01.30, 04.30, 07.30 and 10.00 hours), as well as the corresponding wind speeds in the afternoon as the mean wind speed of three hour

intervals before conducting interpolation in the horizontal direction, thus computing the three hour mean wind velocity when the locus passes through P (Fig. 2). Based on this wind velocity, compute locus segment PP_g for three hours; this is the so-called first guess value. Then at midpoint P_m of the first guess value, by interpolating obtain the mean wind velocity for three hours. According to this wind velocity, eventually compute the locus segment PP_1 passing through point P. Thus, repeatedly the locus of the required length can be computed.

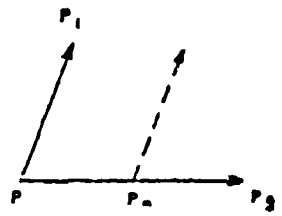

Fig. 2 Schematic diagram showing interpolation values

Figure 3 shows loci of sand dust arrival at Beiling (A), Zhengzhou (B), Jinan (C), Wuhan (D) and Hangzhou (E). Refer to the figure for the corresponding time period that the particular locus spent. From Fig. 3, all loci of the above-mentioned places for 500 and 700 hPa passed through the desert region in the northern part of Xinjiang, the gobi area of the Mongolian Plateau, desert areas of Inner Mongolia, and the loess plateau. However, loci of 500 and 700 hPa passed over some different areas. That is, there are different place of origins for sand dust of two altitudes different from each other. For example, the 500 hPa loci of Wuhan and Hangzhou began in the desert area in the northern portion of Xinjiang, and passed through the southern fringe of the loess plateau. The Beijing 500 hPa locus passed through the desert area of Xinjiang, and some desert areas of Inner Mongolia. Both the Beijing and Jinan 700 hPa loci passed through the gobi area in the southern Mongolian Plateau, and some areas of Inner Mongolia. The Zhengzhou 700 hPa locus crossed the loess plateau.

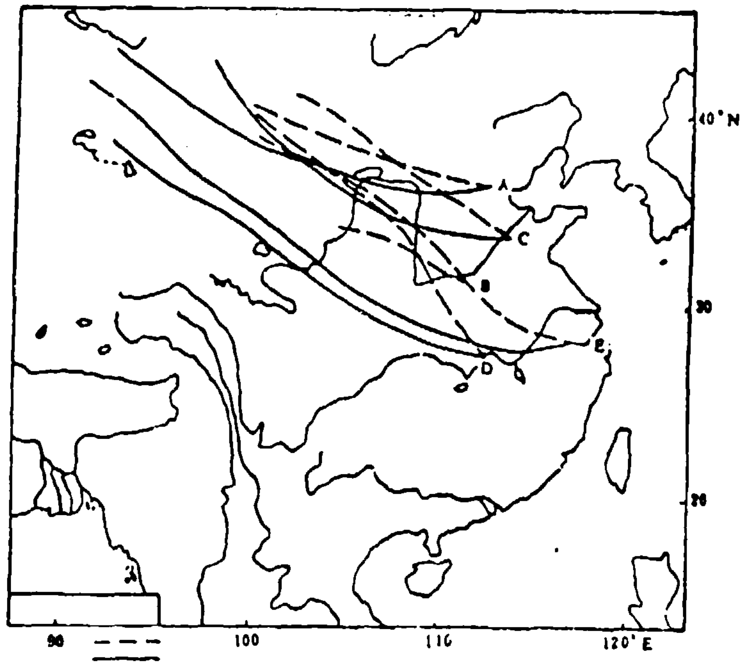

Fig. 3 Loci of sand and dust ---- 700 hPa _____ 500 hPa
In April 1988:

A	Beijing	from 05.00 hours on 10th to 11.00 hours on 11th
B	Zhengzhou	from 02.00 hours on 11th to 14.00 hours on 11th
C	Jinan	from 17.00 hours on 10th to 23.00 hours on 11th
D	Wuhan	from 11.00 hours on 10th to 14.00 hours on 12th
E	Hangzhou	from 08.00 hours on 11th to 20.00 hours on 12th

These loci reveal that there was not a single place of origin of sand and dust. In addition to the desert area in northern Xinjiang where wind originated, areas passed over (desert areas in Inner Mongolia Plateau, and the loess plateau) were also principal place of origins. Both plateaus mentioned above made the highest contribution to this sandstorm weather process. Since the weather process was greatly intensified on the western side of these plateaus, when the frontal surface passed both plateaus, large amounts of sand and dust were swirled upward to transport and distributed toward the lower streams.

This weather process matches the 500 hPa circulation situation. The loci were basically consistent with the routes of movement and directions of the frontal surface and sandstorm weather area.

2. Image discrimination in a satellite cloud map

In a meteorological satellite cloud map, color hues of object images are related to the albedo and solar (altitude) angle. There are different albedos for different substances. On a cloud map, color hues of object images are also different. In the satellite cloud map, black indicates water and land; white indicates clouds; and whitish gray indicates dust storms. Therefore, the place origin and transport routes can be distinguished from images on the satellite cloud map.

Citing Beijing as an example, at 08.00 hours on 10 April, there was a black zone over Beijing in an infrared cloud map. This indicates good sunny weather. At 08.00 hours on 11 April, a white zone was shown over Beijing, indicating a cloud system as no sand and dust were visible from the ground as shown in a weather map. At 11.00 hours on 11 April, there was a gray zone over Beijing, and cloudy weather was shown in a ground weather map. Thus, it is difficult to determine what substance the gray indicates. Actually, floating dust appeared over Beijing after 08.30 hours on that day. At 14.00 hours on 11 April, the expanse of a white cloud system over Beijing moved eastward. There was a whitish gray image (refer to zone B in Fig. 4) in the region approximately between 33° and 45° North and between 105° and 118°; the region includes the Beijing area. However, blue sky was shown in a ground weather map. Apparently, the whitish gray indicates sand and dust. The area covered by whitish gray is consistent with the area covered by the sandstorm and floating dust as shown in a ground weather map. Although to a moderate degree, a sandstorm was still indicated on the cloud map between 17.00 and 20.00 hours. At the same time, whitish gray turned into black in the western portion of the above-mentioned region.

This indicates the phenomenon that the sandstorm had moved eastward; good sunny weather again appeared.

From images on a polar orbit satellite cloud map (not shown in text) on 12 April, the sandstorm had moved out of Beijing, and continued moving southeastward.

Indicating the place of origin of sand and dust, region A in Fig. 4 shows the area of dust cloud KOSA [3] from images taken out of a cloud map presented by the Japan Meteorology Satellite Center. This region was passed by the loci mentioned above. This result is relatively consistent with the authors' analysis. Therefore, based on images in a meteorology satellite cloud map, basically the place of origin and transport direction of sand and dust can be distinguished.

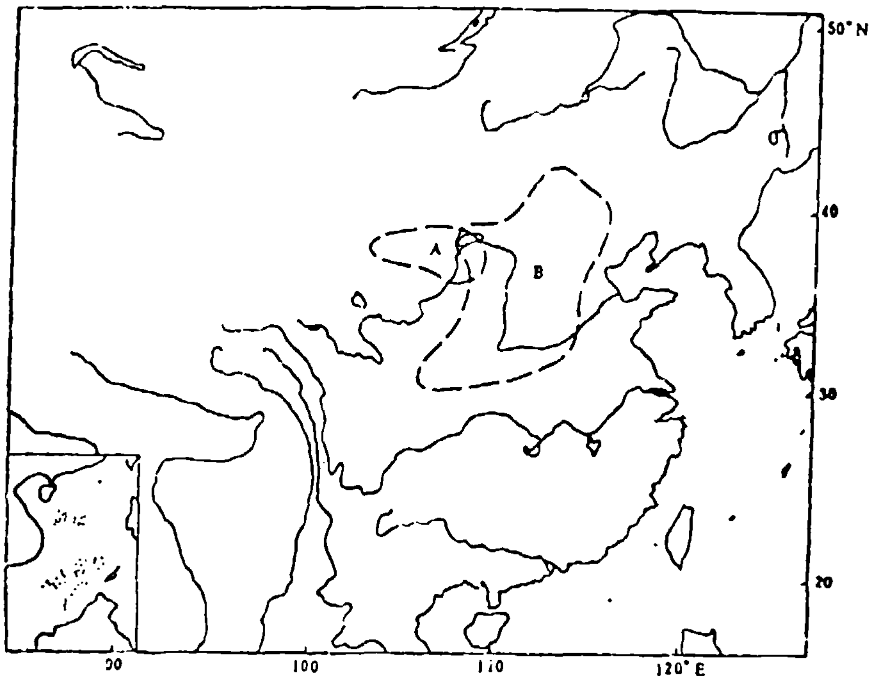

Fig. 4 Satellite cloud map
Zone A is place of origin (from Japan Satellite Meteorology Center); zone B shows the extent of sandstorm and floating dust at 14.00 hours on 11 April (from an infrared cloud map)

3. Analyses of visibility (V) and direct solar radiation (S)

Everywhere reached by the sandstorm, the visibility suddenly dropped and direct solar radiation decreased greatly. Fig. 5 shows the time-space variation of the low visibility (V) region and low direct solar radiation (S) region. The so-called low V value and low S value are relative, indicating the lowest value among all V and S values at different time for a measurement station. Solid and dotted lines in the figure represent, respectively, the low S value region and low V value region. Numbers on an isopleth indicate the time and day the value appears; as S represents daily total insolation, only the day is marked. From the figure, time and scope that low V and low S values show are entirely consistent with the time, scope and route that the front and sandstorm weather zone pass.

Table 1 shows variations of V and S with time at Beijing Municipality. On 9 and 10 April, no sandstorm appeared at Beijing so it was good sunny weather with relatively high V and S values. On 11 April, sandstorm arrived; thus V and S values dropped to the lowest, at 1.2 kilometers and 0.00 MJ/($m^2 \cdot$d) respectively. On 12 April, the sandstorm had left Beijing and weather became better; thus, both V and S values rose with values at 20 kilometers and 13.51 MJ/($m^2 \cdot$d) respectively.

Table 2 lists the time of low V at various measurement stations from west to east. With eastward movement of the sandstorm, time (that V showed) gradually delayed. For example, the time was 20.00 hours on 9 April for Urumqi, 20.00 hours on 9 April for Zhangyi, and 14.00 hours on 11 April for Beijing. Hence, displacements of low V region and low S region, and time that low V showed likewise indicate the place of origin and evolution process of the sandstorm.

Table 1 V (km) and S values (m^2 d) over Beijing from 9 to 13 April

a 项目 \ b 时间	c 9日	d 10日	e 11日	f 12日	g 13日
$\bar{V}$	10.3	7.0	2.6	12.3	18.0
V_{14}	9.0	4.0	1.2	20.0	15.0
S	12.42	1.80	0.00	13.51	15.08

$\bar{V}$ is daily mean value of visibility; V_{14} is the value of visibility at 14.00 hours; S is total daily amount of direct solar radiation.

Key: a - item b - time c - 9th
d - 10th e - 11th f - 12th
g - 13th

Table 2 Time that low V values (km) appeared at various measurement stations

a 地点	b 乌鲁木齐	c 张掖	d 银川	e 呼和浩特	f 北京
g 能见度	6.0	3.0	1.2	4.0	1.2
h 出现时间	9日20时 i	10日20时 j	11日2时 k	11日8时 l	11日14时 m

Key: a - location b - Urumqi
c - Zhangye d - Yinchuan
e - Hohhot f - Beijing
g - visibility h - time of occurrence
i - 20.00 hours on 9th
j - 20.00 hours on 10th
k - 02.00 hours on 11th
l - 08.00 hours on 11th
m - 14.00 hours on 11th

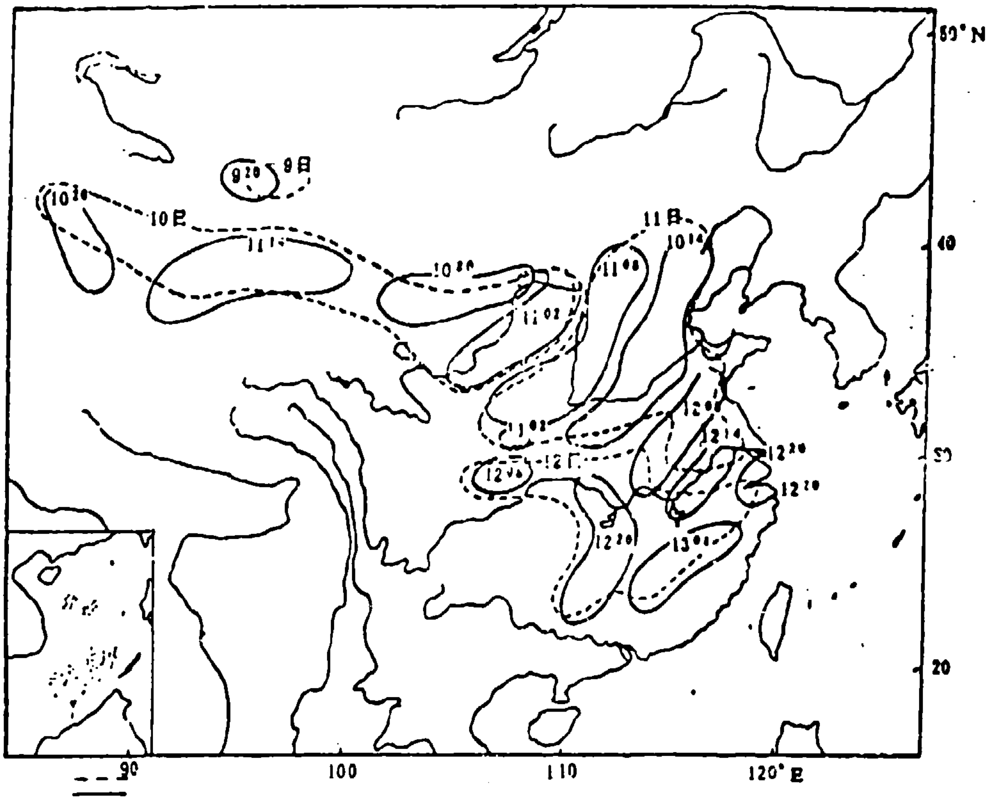

Fig. 5 Zone of low visibility (solid line) and zone of low direct solar radiation (dotted line) from 9 to 13 April 1988

4. Climate and environment of a sandstorm at its place of origin

In areas of China such as Xinjiang, Inner Mongolia and the loess plateau, large amounts of microparticles of sand, dust and loess exist. Since the period from the winter solstice of 1987 to the spring of 1988, the area has suffered a long period of drought with little rainfall; the climate was extremely dry with low moisture content in soil. In Inner Mongolia and the loess plateau, the precipitation was 80 percent lower than for a like period in a normal year. In addition, the plant cover of the area has been continuously damaged with an extremely bare ground

surface. Under such climate background and environmental conditions, once a gale occurs the loess and sand will be blown up by the wind, leading to formation of a sandstorm. This is also one of important reasons leading to this sandstorm weather process.

IV. Physicochemical Characteristics of Sand and Dust

During a sandstorm period, the authors collected sand and dust specimens on 11 April and 12 April at a site about 15 meters in altitude inside the State Meteorology Administration in Beijing, and at Lin'an WMO Background Monitoring Station in Zhejiang Province. At Beijing, a model KB-120 atmosphere sampler was used with a flow rate of 122 to 124 liters per minute, one hour sample collection time, with red light No. 49 glass fiber film. The film was first soaked in nitric acid before rinsing with water. Afterwards, the film was baked at high temperature. At Lin'an, samples were continuously collected for 24 hours by using a large flow rate floating dust sampler (HV-100).

TSP (total suspension particles) of sand and dust was weighed with a balance scale. The element constituents in sand and dust were determined with a plasma emission spectrograph (ICP). The chemical constituents were analyzed with an ion spectrograph. The results are shown as follows.

1. TSP of sand and dust

For sand and dust collected at Beijing, the mean value of TSP is 5118 micrograms per square meter. The value is 15.7 times higher than that under normal weather conditions, and 2.4 times higher than that collected at Lin'an with the same process. During the sandstorm period at Lin'an, the TSP is 14.7 times higher than that under normal weather conditions. At Beijing and Lin'an during normal weather conditions, the TSP is 306 and 97 micrograms per square meters, respectively. It is apparent that

the transport quantities of sand and dust during this sandstorm weather process are quite high.

2. Determination of elements in sand and dust

In three specimens collected at Beijing, 21 elements were detected (see Table 3). Divided according to mean value of element concentrations, those with element concentration greater than 500 parts per million are Al, Fe, K, Mg, S, P, Ti and Na. Those with element concentration between 100 and 500 parts per million are Mn, Ba and V. Those with element concentration between 1 and 100 parts per million are Zn, Ni, Pb, Vr, Co and Cd. Other elements were not detected. In three specimens, the same elements are not detected. This may be due to uneven distribution of background value of elements for the film.

Table 3 Concentrations (ppm) of elements in sand and dust

元素 a	样品 (1) b	样品 (2) b	样品 (3) b	平均值 c	元素 a	样品 (1) b	样品 (2) b	样品 (3) b	平均值 c	元素 a	样品 (1) b	样品 (2) b	样品 (2) b	平均值 c
Ba	24	456	219	233	Mg	27	13884	3811	5841	V	19	178	132	110
Ca	—	8964	—	—	Mn	81	780	603	488	Zn	—	64	12	38
Cd	—	11	2	7	Na	259	1350	720	776	B	—	1188	—	—
Co	3	27	17	16	Ni	8	44	36	28	Li	—	40	—	—
Cr	7	64	47	39	Pb	4	45	23	24	P	166	1952	1384	1167
Cu	—	—	—	—	Al	3789	91813	39474	44959	S	391	2825	1941	1719
Fe	4250	34092	28842	22395	Sr	—	254	—	—	Sn	—	175	—	—
K	2018	16492	13803	10771	Ti	147	1282	911	780					

In the table, __ indicates that the value of the particular elements falls below the detection limit.

Key: a - element b - sample c - mean value

Of the element concentration values of sand and dust, those elements with high values are Al, Fe, K, Mg, Ti and Mn; these elements are some of the eight major elements with affinity to rock [6]. Si was not detected due to restrictions in instrument conditions. The value of Ca is quite high at 8960 parts per million in specimen No. 2; the value is close to the background value in the Earth's crust. Therefore, the authors can preliminarily conclude that elements in sand and dust are mainly from natural source with little effect from human pollution.

3. Enrichment conditions of elements in sand and dust

Enrichment of elements is closely related to physicochemical properties and the place of origin. Owing to different places of origin and formation conditions, the enrichment of different elements is apparently different. Therefore, based on the enrichment extent of an element, we can determine whether it comes from a natural source or from a source discharged by humans.

Of the Mason values, in this article Fe and Ti are used as elements for reference and comparison. The computation equation for the enrichment factor is as follows.

$$EF_{(Fe)} = \frac{(x/Fe)_{a}}{(x/Fe)_{b}} \quad (1)$$

Key: a - sand and dust; b - Earth crust

In the equation, $EF_{(Fe)}$ is the enrichment factor using Fe as the element for reference and comparision. The subscripts sand and dust in one case, and the Earth's crust in another indicate that enrichment values of x and Fe in specimens of sand and dust are taken, respectively, from determining values in sand and dust, and from average abundance in the Earth's crust. Computation results of enrichment factor of various elements are listed in Tables 4 and 5. In three specimens, the determination values of Cd, Pb, B and Sn are different by orders of magnitude.

This is possibly because of uneven distribution of background values on film, or due to some errors. Such a difference is not representative so it is not discussed in the article.

According to Table 4 and Table 5, the mean value of the enrichment factor of elements has the following features: a) for the same element, $EF_{(Ti)}$ is higher than $EF_{(Fe)}$; b) there is only one element S whose EF value is greater than 10; its $EF_{(Ti)}$ and $EF_{(Fe)}$ values are 39.45 and 15.52, respectively. c) The EF value of all other elements is smaller than 10; most of these values are close to 1. In particular, more elements with Fe as the element for reference and comparison have an EF value close to 1, such as Al, Fe, Mg, Mn, Zn, and Ni. d) The EF value of Ti and Na is considerably smaller than 1.

Table 4 Enrichment factors (EF) of element in sand and dust

a 元素	b 样品(1)	b 样品(2)	b 样品(3)	c 平均值	a 元素	b 样品(1)	b 样品(2)	b 样品(3)	c 平均值	a 元素	b 样品(1)	b 样品(2)	b 样品(3)	c 平均值
Ba	0.66	1.57	0.89	1.04	Mg	0.02	0.98	0.32	0.43	V	1.66	1.93	1.70	1.7[illegible]
Cs	—	0.36	—	—	Mn	1.00	1.20	1.10	1.10	Zn	—	1.34	0.30	
Cd	—	80.66	17.34	49.00	Na	0.11	0.07	0.04	0.07	B	—	174.23	—	
Co	1.41	1.58	1.18	1.39	Ni	0.78	0.86	0.83	0.82	Li	—	2.93	—	—
Cr	0.82	0.94	0.81	1.86	Pb	3.62	5.08	3.07	3.92	P	1.86	2.73	2.29	2.29
Cu	—	—	—	—	Al	0.55	1.65	0.84	1.01	S	17.69	15.94	12.94	15.62
Fe	1.00	1.00	1.00	1.00	Sr	—	0.89	—	—	Sn	—	128.33	—	—
K	0.92	[illegible]	0.92	0.92	Ti	0.38	0.43	0.36	0.39					

In the table, __ indicates that the value of the particular element falls below the detection limit. Fe is the element for reference and comparison.

Key: a - element b - sample c - mean value

Table 5 Enrichment factors (EF) of element in sand and dust

a 元素	b 样品 (1)	b 样品 (2)	b 样品 (3)	c 平均值	a 元素	b 样品 (1)	b 样品 (2)	b 样品 (3)	c 平均值	a 元素	b 样品 (1)	b 样品 (2)	b 样品 (3)	c 平均值
Ba	1.69	3.68	2.49	2.62	Mg	0.04	2.25	0.88	1.06	V	4.21	4.53	4.72	4.49
Ca	—	0.85	—	—	Mn	2.55	2.82	3.07	2.81	Zn	—	3.14	0.85	1.99
Cd	—	188.77	34.32	74.36	Na	0.27	0.16	0.12	0.18	B	—	407.74	—	—
Co	3.60	3.71	3.28	3.53	Ni	2.00	2.01	2.32	2.11	Li	—	608.60	—	—
Cr	2.10	2.20	2.27	2.19	Pb	9.21	11.88	8.50	9.86	P	4.73	6.38	6.37	5.83
Cu	—	—	—	—	Al	1.39	3.86	2.35	2.53	S	45.00	37.29	36.06	39.45
Fe	2.54	2.34	2.79	2.56	Sr	—	2.32	—	—	Sn	—	300.31	—	—
K	2.33	2.19	2.57	2.36	Ti	1.00	1.00	1.00	1.00					

In the table, __ indicates tnat the value of the particular element falls below the detection limit. Fe is the element for reference and comparison.

Key: a - element b - sample c - mean value

Since there is no particle gradation for specimens of sand and dust, it is difficult to determine whether those elements with EF greater than 10 are affected by human pollutic or if those elements with EF less than 10 are from natural source. However, from the record that the EF value of S is in excess of 100 [6] in dust particles over Be..i'.g collecte' at times other than sandstorm weather, the EF value during the ind..or heating period is even higher. In this sandstorm weather, the $EF_{(Fe)}$ value of S is only 15.52, which is not a high value. Thus, the pollution effect is very small. However, the EF value of other elements is close to the mean abunda..ce in Earth's crust. Thus, we can conclude that elements in sand and dust are mainly from natural sources.

4. Chemical constituents in sand and dust

Refer to Table 6 for determination results of chemical constituents of sand and dust collected at Beijing and Lin'an.

Table 6 Concentrations of chemical constituents in sand and dust (micrograms per cubic meter)

样品 a	F^-	Cl^-	NO_3^-	$SO_4^=$	NH_4^+
北京 b (黄沙)	0.72	5.61	2.38	15.01	2.27
临安 c (黄沙)	0.28	4.35	4.83	28.03	0.94
临安 d (正常天气)	0.24	2.27	2.70	27.76	0.64

Key: a - sample b - Beijing (sand)
c - Lin'an (sand)
d - Lin'an (normal weather)

In the table, F^-, Cl^- and NH^+ are higher for specimens collected at Beijing than those collected at Lin'an. The NO^- and [illegible] are higher at Lin'an than those at Beijing. Compared to the value in normal weather at Lin'an, the Cl^- and NO^- are slightly higher in the sandstorm weather period, other chemical constituents are not much different for different weather conditions. The reason for high values of NO^- and SO^- at Lin'an is possibly related to the effect of large amounts of industrial discharges from middle and small sized enterprises.

V. Preliminary Conclusion

From the above-mentioned analyses and studies, the authors can preliminarily reach the following conclusions: (1) The direct cause of this intensive sandstorm weather process is eastward movement of two large European troughs, leading to vigorous activities of a very cold air mass which penetrated China. (2) The transport route of sand and dust in the atmosphere was mainly

eastward and southeastward; the transport and diffusion were from the west and northwest. Beginning on 12 April over the 850 hPa, there was an intensive air flow from the northeast over Nanjing, Wuhan, Nanchang, Changsha and Guilin; thus part of the sand and dust turned to transport southwestward. (3) For the place of origin of sand and dust, in addition to the desert area in northern Xinjiang where the wind originated, on the route the various desert areas of Inner Mongolia, gobi and the loess plateau were also the major places of origin for this sandstorm with the greatest contribution. (4) Since the weather process of this sandstorm was very intense with high wind velocity, transport and diffusion of pollutants in the atmosphere were also very intense with very little human pollution effect on elements in sand and dust with the principal origin from natural sources.

A first draft of the article was received on 2 September 1989; the final, revised draft was received for publication on 17 December 1989. The authors are grateful to Comrade Wang Chao of the data laboratory of the State Meteorology Administration, and Comrade Dong Liqing of the Central Weather Observatory for their assistance.

REFERENCE

[1] Darzl, M. D., and W. Winchester, Aerosol characteristics at Mauna Loa observatory, Hawii, after east Asian dust storm episodes, *J. Geophys. Res.*, 87, 1251-1258, 1982.

[2] Muragame, N., Dust cloud "kosa" from the east Asian dust storm in 1982-1988 as observed by the GMS satellite, Japan Met. Satellite Centre Technical Report, NO. 17, 1988.

[3] Swasaka, y., M. Yamato, R. Jmasu and A. Ono, Transport of Asian dust (KOSA) particles, importance of weak KOSA events on the geochemical cycle of soil particles, *Tellus*, 40 B, 491-503, 1988.

[4] Qu Shaoyuan, Li Yuying, Zhou Mingyu, Yang Shaojin, and Qian Qinfang, "Origin of Sand and Dust in a Sandstorm Weather Process Over the Beijing Area," HUAIJING KEXUE XUEBAO [JOURNAL OF ENVIRONMENTAL SCIENCE], 4, No. 1, 1984.

[5] Haris, J. M., "The GMCC Atmospheric Trajectory Program," NOAA Technical Memorandum, ERL-116, 1982.

[6] Wang Anpu et al., "Chemical Properties of Atmospheric Floating Dust Over the Beijing Area," JOURNAL OF ENVIRONMENTAL SCIENCE, 1, 3, 1981.

DISTRIBUTION LIST

DISTRIBUTION DIRECT TO RECIPIENT

ORGANIZATION	MICROFICHE
B085 DIA/RTS-2FI	1
C509 BALLOC509 BALLISTIC RES LAB	1
C510 R&T LABS/AVEADCOM	1
C513 ARRADCOM	1
C535 AVRADCOM/TSARCOM	1
C539 TRASANA	1
Q592 FSTC	4
Q619 MSIC REDSTONE	1
Q008 NTIC	1
Q043 AFMIC-IS	1
E051 HQ USAF/INET	1
E404 AEDC/DOF	1
E408 AFWL	1
E410 ASDTC/IN	1
E411 ASD/FTD/TTIA	1
E429 SD/IND	1
P005 DOE/ISA/DDI	1
P050 CIA/OCR/ADD/SD	2
1051 AFIT/LDE	1
P090 NSA/CDB	1
2206 FSL	1

Microfiche Nbr: FTD93C000643
FTD-ID(RS)T-0331-93